BIOCHEMICAL PHARMACOLOGY 73 (2007) 259–269

available at www.sciencedirect.com

ScienceDirect

journal homepage: www.elsevier.com/locate/biochempharm

Molecular cloning, mutations and effects of NK_1 receptor antagonists reveal the human-like pharmacology of gerbil NK_1 receptors

Susanna Engberg, Ingela Ahlstedt, Agnes Leffler, Erik Lindström, Elin Kristensson, Arne Svensson, Ingrid Påhlman, Anders Johansson, Tomas Drmota, Bengt von Mentzer *

AstraZeneca Research & Development, 431 83 Mölndal, Sweden

ARTICLE INFO

Article history:
Received 3 August 2006
Accepted 28 September 2006

Keywords:
Gerbil
Neurokinin 1 receptor cloning
Nueurokin receptor antagonists
Site directed mutagenesis
Gerbil foot tap
Homology models

ABSTRACT

The present study investigates the pharmacology of the cloned neurokinin 1 receptor from the gerbil (gNK_1R), a species claimed to have human-like NK_1R (hNK_1R) pharmacology.

The amino acid sequence of NK_1R was cloned. The hNK_1R, rat NK_1R (rNK_1R), gNK_1R and mutants of the gNK_1R were expressed in CHO cells. The affinity and potency of NKR agonists and the NK_1R antagonists CP99994 and RP67580 (NK_1R-selective) and ZD6021 (NK1/2R) were assessed *in vitro* by monitoring [^{3}H]-SarMet SP binding and substance P-evoked mobilization of intracellular Ca^{2+}. The gerbil foot tap (GFT) method was used to assess the potency of the antagonists *in vivo*.

The gNK_1R coding sequence displayed an overall 95% and 97% homology with hNK_1R and rNK_1R, respectively. The affinity of the NK_1R-selective agonist ^{3}H-SarMet SP for human and gerbil NK_1R was similar (2.0 and 3.1 nM) but lower for rNK_1R (12.4 nM). The rank order potency of the agonists for NK_1R was SP $\geq$ ASMSP $\geq$ NKA $\ggg$ pro7NKB in all species. The NK_1R antagonists, ZD6021 and CP99994, had comparable affinity and potency for gerbil and human NK_1R, but were 1000-fold less potent for rNK_1R. In contrast, RP67580 had comparable affinity and potency for all three species. Mutations in positions 116 and 290 did not affect agonist potency at the gNK_1R while the potency of the antagonists ZD6021 and CP99994 were markedly decreased (10–20-fold). It is concluded that gNK_1R has similar antagonist pharmacology as the human-like orthologue and that species differences in antagonist function depend on key residues in the coding sequence and antagonist structure.

* *Corresponding author at*: Molecular Pharmacology, AstraZeneca Research & Development, 431 83 Mölndal, Sweden. Tel.: +46 31 7761716; fax: +46 31 7763761.
E-mail address: bengt.mentzer@astrazeneca.com (B. von Mentzer).

Abbreviations: NK, neurokinin; SP, substance P; NKA, neurokinin A; Pro7NKB, [Pro^7]-neurokinin B; ASMSP, acetyl-[Arg^6,Sar^9,Met(O$_2$)^{11}]-SP6-11; NK_1R, neurokinin 1 receptor; gNK_1R, gerbil neurokinin 1 receptor; hNK_1R, human neurokinin 1 receptor; rNK_1R, rat neurokinin 1 receptor; mNK_1R, mouse neurokinin 1 receptor; $gpNK_1R$, guinea pig neurokinin 1 receptor; GFT, gerbil foot tap; Ile, isoleucine; CHO, Chinese Hamster Ovary; HPLC, high performance liquid chromatography; LC–MS, liquid chromatography–mass spectrometry; MRM, multiple reaction monitoring

0006-2952/$ – see front matter
doi:10.1016/j.bcp.2006.09.030

1. Introduction

The structurally related tachykinins substance P (SP), neurokinin A (NKA) and neurokinin B (NKB) are the well-known mammalian members of the tachykinin peptide family [1]. Recently, additional mammalian tachykinins such as hemokinin-1 and endokinins have been discovered [2]. The tachykinins mediate their effects via binding to G-protein-coupled neurokinin (NK) receptors [3–5]. The NK receptor subtypes cloned and characterized so far are termed NK1 (NK_1R), NK_2 (NK_2R) and NK_3 (NK_3R). SP has the highest affinity for the NK_1R and NKA and NKB for the NK_2R and NK_3R, respectively. However all three tachykinins can interact with each receptor.

The NK_1R has been considered as an attractive target in a wide-variety of indications such as asthma, pain, psychiatric disorders, emesis, gastrointestinal disorders and urine incontinence [6–9] resulting in the development of several NK_1R-selective antagonists [10,11].

Interestingly, species-related variations exist in the primary sequence of the NK_1R which affect the affinity of small-molecule NK_1R antagonists without affecting the potency or efficacy of endogenous agonists [12]. The NK_1R family can be grouped into two sub-families based on receptor orthologues affinity to small molecule antagonists. The first sub-family consists of the human, guinea pig, rabbit, dog, gerbil and ferret NK_1R, while the second sub-family consists of rat and mouse NK_1R [13,14]. The cloned rat and human NK_1R (rNK_1R and hNK_1R) display 95% homology over the whole amino acid sequence. However, when analyzing the seven transmembrane regions, six amino acids differ between the two species. In contrast, the guinea pig NK_1R (gp NK_1R), a species with similar NK_1R antagonist pharmacology to man, has 97% homology overall and is 100% identical in the transmembrane regions to hNK_1R. Hence, the degree of homology in the transmembrane regions between different species may predict if similarities exist in antagonist pharmacology. Indeed, previous reports indicate that residues 116 and 290, located in transmembrane (Tm) regions 3 and 7, respectively, are important in dictating the species selectivity between rNK_1R and hNK_1R at least when it comes to the NK_1R antagonists RP67580 and WIN 51708, both having a higher affinity for rNK_1R [15,16] and CP96345, CP99994 and FK888, having a higher affinity for hNK_1R [15,17–19].

Due to the differences in NK_1R orthologoue pharmacology, several non-rat/mouse models have been developed to screen for potency and efficacy of NK_1R small molecule antagonists *in vivo*. Gerbils belong to the human sub-family and therefore represent a relevant animal species for identifying clinically active NK_1R antagonists. One assay often used is the so-called gerbil foot tap model (GFT) [20]. Central (intracerebroventricular, i.c.v.) administration of selective NK_1R agonists results in repetitive hindfeet tapping of the gerbil. Pretreatment with potent NK_1R antagonists that have the capability to pass the blood brain barrier inhibit agonist-induced foot tapping. This model has been useful in screening for small molecule antagonists possessing central activity [6,20–24]. In addition, the GFT model has been used to predict anti-emetic properties of NK1R antagonists [21] and to predict occupancy of centrally located NK_1R [25]. Gerbils have also been used in behavioural models intended to identify potential anti-depressant or anxiolytic effects of NK_1R antagonists [26,27].

In contrast to human, rat and gpNK_1Rs, the gerbil NK_1R (gNK_1R) has not been cloned. The similarities in affinity between human and gNK_1R have only been shown using binding experiments from gerbil tissues [13]. The aims of this study were to clone the gNK_1R, provide pharmacological characterization, and to identify key positions for antagonist affinity and function using site-directed mutagenesis.

2. Materials and methods

2.1. Chemicals

Acetyl-[Arg^6,Sar^9,$Met(O_2)^{11}$]-SP6-11 (ASMSP), a selective NK1-receptor agonist, SP, NKA and Pro7NKB were purchased from Bachem (Peninsula Laboratories Inc., San Carlos, CA). 3-Cyano-naphthalene-1-carboxylic acid ((S)-2-(3,4-dichloro-phenyl)-4-{4-[2-((S)-methanesulfinyl)-phenyl]-piperidin-1-yl}butyl)-methyl-amide (ZD6021), (2-methoxy-5-trifluoromethoxy-benzyl)-((2S,3S)-2-phenyl-piperidin-3-yl)-amine (CP99994) and (3aR,7aR)-2-[1-imino-2-(2-methoxy-phenyl)-ethyl]-7,7-diphenyl-octahydro-isoindol-4-one (RP67580) were all synthesized at AstraZeneca Wilmimgton, USA [28–30].

2.2. Molecular cloning and mutagenesis of the NK1 receptor

Total RNA was prepared from 20 to 100 mg of gerbil pancreas and striatum with RNA-STAT-60 (Tel-Test Inc., Texas) and used as sources for NK1 receptor (NK_1R) cloning. One microgram of total RNA from striatum and pancreas respectively were used for the first strand cDNA synthesis using SMART RACE cDNA Amplification kit (BD Biosciences, NJ). ClustalW alignment of NK_1R sequence from human, rat, mouse and guinea pig was used to select primers with high homology between different species. Primers used in the 3′RACE and in the 5′RACE are shown in Table 1. The RACE reactions were performed on cDNA from gerbil pancreas. The RACE fragments were characterized and two clones containing gerbil specific NK1 sequence in the untranslated region were identified. Full-length PCR was performed using gerbil specific primers (Table 1). Complementary DNA from striatum (2.5 μl) was used in the optimized full-length PCR with forward and reversed primer (1× PCR buffer, 5 mM of each dNTP, 20 μM primers and 1 U Pfu Ultra, Stratagene, La Jolla, CA). Optimized conditions were incubation for 2 min at 95 °C followed by 35 cycles at 95 °C denaturation for 30 s, 55 °C annealing for 1 min, 72 °C extension for 2 min followed by an extension step at 72 °C for 10 min. The resulting PCR product was cloned into pCR®4Blunt-TOPO vector (Invitrogen, Carlsbad, CA, USA) and 10 different clones were sequenced. The consensus sequence was used to design new primers containing restriction sites (Table 1) used in a new PCR for sub cloning in the pIREShyg2 expression vector (BD Biosciences Clontech, Paolo Alto, CA, USA).

All mutations were made using the Quick-Change Multi Site-Directed Mutagenesis Kit (Stratagene, La Jolla, CA). The

Table 1 – Primers used for the gerbil NK_1R cloning and mutagenesis

Step	Primers
SMART RACE	5′-GCTGCCCTTCCACATCTTCTTCCTCCTG-3′ (3′RACE) 5′-GCCAGCAGGAGAGCCAGGACCCAGATG-3′ (5′RACE)
Full-length PCR	5′-AGGCATCTGCAACAAGGTC-3′ (forward) 5′-AACCATTATGACCCTTTCCAGA-3′ (reverse)
Subcloning	5′-GGATCCGCCACCATGGATAACGTCCTCCCTGG-3′ (forward, *Bam*HI, Kozac sequence) 5′-GATATCATGCCCTTGAAATATGCCCACTG-3′ (reverse, *Nhe*I)
Mutation 1 (M54I)	5′-CAACGTGGTGGTGAT**A**TGGATCATTTTGGC-3′
Mutation 2 (S80C)	5′-GCTGAGGCCT**G**CATGGCCGCATTC-3′
Mutation 3 (V116L)	5′-CCATTGCTGCT**C**TCTTCGCCAGCATC-3′
Mutation 4 (I290S)	5′-TCTACCTGGCCA**G**CATGTGGCTAGCC-3′

The Kozac sequence is italicised and mutations are indicated in bold.

gerbil NK_1R in the pIREShyg2 expression vector was used as a template in all reactions. Four single mutations were made together with one construct combining all four single mutation (Table 1). All primers used were ordered from Qiagen (http://www.oligos.qiagen.com).

2.3. Cell culture and transfection

Chinese Hamster Ovary (CHO) cells (obtained from ATCC, Middlesex, UK) were transfected with rat (accession number J05097), gerbil (accession number AJ884917) or mutated gerbil NK_1R, using Lipofectamine™ 2000 (Invitrogen, CA). Clones expressing rat NK_1R or gerbil NK_1R (wt or mutated) were selected by growth in 500 μg/ml hygromycin B and tested for functionality in a Ca^{2+} mobilization assay. CHO cells stably expressing human NK_1R (accession number NM_001058) was supplied by AstraZeneca R&D, Wilmington, USA. Stable transfectants were maintained by supplementing culture media (NutMix F12 (HAM) with Glutamax I, 10% FBS) with hygromycin B at 500 μg/ml for rat and gerbil NK1 (wt or mutated) expressing cells or geneticin at 200 μg/ml for human NK1 expressing cells. Cultures were kept at 37 °C in a 5% CO_2-incubator and routinely passaged when 70–80% confluent for up to 20–25 passages.

2.4. Membrane preparations

CHO-cells expressing human, rat or gerbil (wt or mutated) NK_1R were detached with Accutase® and harvested in ice-cold PBS. The cells were washed twice in PBS, pelleted by centrifugation for 5 min at 1500 rpm and re-suspended in 20 volumes of lysis buffer (Tris–HCl 50 mM, EDTA 10 mM, Complete EDTA-free protease inhibitor cocktail tablets 20 pills/l (Roche, Mannheim, Germany), pH 7.2 at 4 °C). Cells were homogenized with an UltraTurrax for 2×15 s at 14,000 rpm followed by centrifugation $1000 \times g$ for 10 min at 4 °C. The pellet was resuspended in lysis buffer and homogenized once more. The homogenized cells were recentrifuged at $1000 \times g$ for 10 min at 4 °C. The supernatants were pooled together and centrifuged at $70{,}000 \times g$ for 30 min at 4 °C. The membrane pellet were resupended in freezing buffer (10 mM Tris–HCl, 1 mM EDTA, 10% sucrose), aliquoted and stored at −80 °C. The protein concentrations were determined using a Bio-Rad kit with lyophilized bovine plasma gamma globuline as standard [31].

2.5. Receptor binding assay

The radioligand binding assay was performed at room temperature in 96-well microtiter plates (Low binding, Corning, NY, USA). The saturation binding experiments were performed in the concentration range 0–50 nM, and 10–50 μg of membrane was mixed with serial dilutions of [prolyl2,4-3,4(*n*)-^{3}H] Substance P (Amersham Biosciences, Buckinghamshire, UK) or Substance P (9-SAR, 11-Met (O_2)), [2-propyl-3, 4, -^{3}H] (Perkin-Elmer, MA, USA) in incubation buffer (50 mM Tris–HCl, 0.1% BSA, 40 mg/l bacitracin, Complete EDTA-free protease inhibitor cocktail tablets 20 pills/l (Roche) and 3 mM $MnCl_2$) and incubated for 30 min on a microtiter plate shaker. In displacement binding 4 nM of ^{3}H SarMet was used. Non-specific binding was determined in the presence of 10 μM ZD6021 [22]. The membranes were collected by rapid filtration on filtermats (pre-treated with 0.3% polyethyleneimine) using a Micro96 Harvester (Molecular Devices, UT, USA). Filters were washed by the harvester with ice-cold wash buffer (50 mM Tris–HCl, 3 mM $MnCl_2$ pH 7.4 at 4 °C) and dried at 55 °C for 30–60 min. Meltilex scintillator sheets were melted on to the filters using a Microsealer (Wallac, Turku, Finland). The filters were counted in a β-Liquid Scintillation Counter (1450 Microbeta Trilux, Wallac, Turku, Finland).

2.6. Calcium mobilization assay

Ca^{2+} mobilization was studied using a Fluorometric Imaging Plate Reader, FLIPR™ or FlexStation (Molecular Devices) in CHO cells stably expressing human, rat or gerbil NK1 receptors. Cells were seeded into black walled clear-base 96-well plates (Costar®3904, Corning Inc., NY, USA) at a density of 35,000 cells per well in culture media and grown for approximately 24 h in a 37 °C CO_2-incubator. In FLIPR experiments, the cells were incubated with the cytoplasmic Ca^{2+} indicator Fluo-4 (Teflabs 0152, Austin, USA) at 4 μM in loading media (Nut Mix F12 (HAM)) with Glutamax I, 22 mM HEPES, 2.5 mM probenicid (Sigma, P-8761) and 0.04% Pluronic F-127 (Sigma P-2443) for 30 min in a 37 °C CO_2-incubator. The Fluo-4-loaded cells were then washed three times in assay buffer

(Hanks Balanced Salt Solution, 20 mM HEPES, 2.5 mM probenicid and 0.1% BSA). The plates were then placed into the FLIPR^{TM} to monitor cell fluorescence (λ_{ex} = 488 nm, λ_{em} = 540 nm) before and after the addition of antagonists and/or agonists. Antagonists and agonists were dissolved in assay buffer (final DMSO concentration kept below 1%) on 96-well plates and added to the loaded cells by the automated pipettor in the FLIPR^{TM}. Loaded cells were pre-incubated with antagonists for approximately 2 min before addition of agonist. Ca^{2+} mobilization responses were measured as peak fluorescence intensity minus basal fluorescence after agonist addition. Experiments performed on FLEX station were made using ''Calcium assay kit'' (#R8033; Molecular Devices), according to manufacturers instructions. Cells were washed with HBSS/Hepes (20 mM, pH 7.4) and then incubated for 45–60 min at 37 °C with 150 μl assay buffer per well: calcium assay kit reagent dissolved in HBSS/Hepes, 2.5 mM probenecid was included in the assay buffer. Loaded cells were pre-incubated with antagonists for 2–15 min before addition of Substance P (0.08 nM). Agonist was automatically added in both the FLIPR and FLEX station setup.

2.7. *Gerbil foot tap*

Male Mongolian gerbils (60–80 g) were purchased from Charles River (Sulzfeld, Germany). On arrival, they were housed in groups of 10 in cages (height: 40 cm, width: 80 cm, length: 60 cm) containing an enriched environment including hay, plastic tubes, nesting material and sand. Food and water were available *ad libitium* and the cages were placed in temperature and humidity-controlled holding rooms. The animals were allowed at least 7 days to acclimatize to the housing conditions before experiments. All experiments were approved by the local animal ethical committee of Göteborg, Sweden.

Compounds and corresponding vehicles were administered under brief isoflourane (Forene®) anaesthesia. Fig. 1 shows the chemical structures of the used NK_1R antagonists. A dose of 10 μmol/kg RP67580 or ZD6021 (dissolved in 28% cyclodextrin) was administered intraperitoneally (i.p.) 30 min prior to the experiment while 1 μmol/kg of CP99994 (dissolved in saline) was administered subcutaneously (s.c.) 1 h before the experiment. 30–60 min later, the animals were anaesthetised again (isoflourane), and a small incision was made in the skin over bregma. 10 pmol of acetyl-[Arg^6,Sar^9,Met(O$_2$)^{11}]-SP6-11 (ASMSP), a selective agonist for NK1 receptors, was administered i.c.v. in a volume of 5 μl using a Hamilton syringe with a needle 4.5 mm long. The wound was clamped shut and the animal was allowed to recover in a small plastic cage. The cage was placed on a piece of plastic tubing filled with water and connected to a computer via a pressure transducer. The number of taps produced by the animal were recorded for 6 min using customized computer software (PharmLab on-line 4.0, AstraZeneca, Mölndal, Sweden). The average number of taps per minute during the middle 5 min were calculated (thus the first and last 30 s were excluded). Ten pico mole of ASMSP typically evoked an average of 100 taps per minute. Antagonist efficacy was expressed as % inhibition in comparison to corresponding vehicle. After the experiment, the animals were sacrificed under anaesthesia by exsanguination of the heart. The brain was removed in order to determine levels of compound.

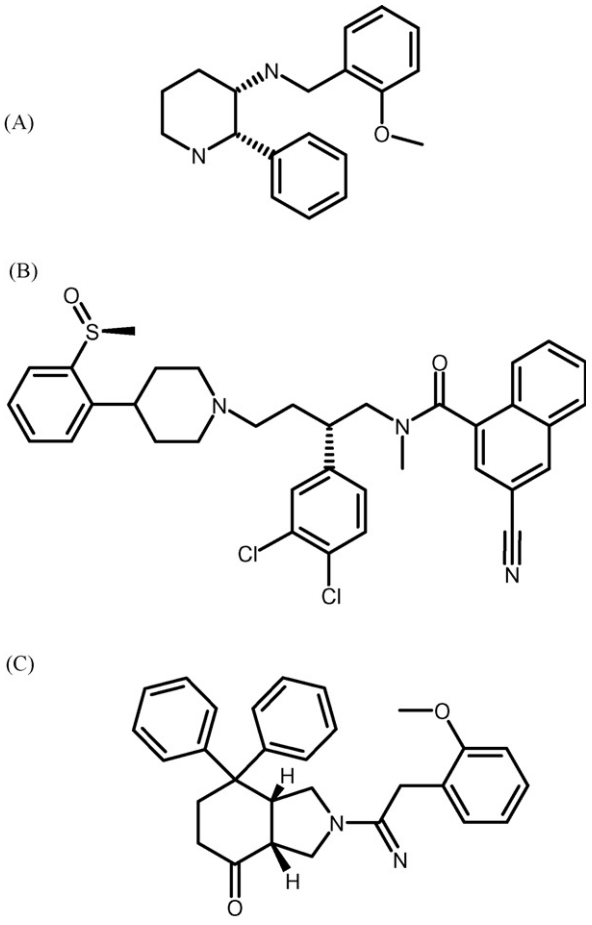

Fig. 1 – Chemical structures of antagonists evaluated in the present study: (A) CP99994, (B) ZD6021 and (C) RP67580.

2.8. *Analysis of NKR antagonists*

The brain was collected at the end of the experiment and frozen on dry ice. The brain was thawed and wet weight recorded and diluted by weight in 3 ml of water and sonicated for 30 s and kept on ice. The analytical method for quantitative determination of brain tissue concentration was based on protein precipitation, HPLC separation (Agilent 1100, gradient pump) and the compounds were detected by a tripple quadrupole masspectrometer (Waters, Quattro LC) with positive electrospray ionisation and MRM (Multiple Reaction Monitoring) acquisition.

Fifty microliters of brain homogenate was precipitated with 150 μl cold acetonitrile. The samples were centrifuged for 20 min at 4 °C and 4000 rpm. Seventy-five microliters of the supernatant was diluted with 75 μl of 0.2% formic acid and 10 μl of the extract was injected into LC–MS system. The compounds were separated from other components on a short reversed phase analytical column (HyPURITY C18, 5 μm, 2.1 mm × 30 mm) with rapid gradient elution from 4 to 90% mobile phase B in 2 min held at 90% for 1 min and returned to

initial condition in one step. The pre-column used was Zorbax Eclips XDB-C8, 5 μm, 2.1 mm × 12.5 mm with a mobile phase A consisting of 0.2% formic acid and 2% acetonitrile and mobile phase B consisting of 0.2% formic acid in acetonitrile. The gradient was 4–90% B in 2 min, held at 90% for 1 min and returned to initial condition in one step (flow rate 0.4–0.6 ml/min) with a 20 μl loop (injection volume 5–10 μl). The quantification of the samples were performed using standard curve fitting with linear or quadratic regression. The retention time ranged from 1.0 to 1.9 min using flow rates of 0.6 and 1.2 ml/min, respectively.

2.9. Rhodopsin homology model

The sequences of the human NK_1R were aligned to bovine rhodopsin and a subset of rhodopsin sequences, covering different degrees of sequence identity. The pair wise alignments of NK_1R and rhodopsin, were extracted and adjusted manually to optimize compatibility with structure and frequently occurring sequence motifs amongst GPCRs. The rhodopsin NK1 alignment was used as input for the automatic modelling using the Whatif package [32]. The model was evaluated using the WhatCheck module [32]. A limitation of the Whatif modelling tool is that insertions and gaps are not considered. In this case, however, the active site should not be affected by this limitation.

2.10. Data analysis

Data generated *in vitro* were fitted to a four parameter equation using Excel Fit IDBS software. IC_{50}s were determined from 10-point concentration–response curves for each compound. The agonist potency values are expressed as EC_{50}-values. The affinity (K_i) and potency (K_B)-values for antagonists were calculated using the Cheng–Prusoff equation [33] and expressed as pK_i and pK_B-values (p$K_i = -\log K_i$). The affinity of the used radioligands is expressed as K_d-values and maximal number of receptors as B_{max}-values. All *in vitro* data are expressed as mean ± S.D. and all *in vivo* data are expressed as mean ± S.E.M.

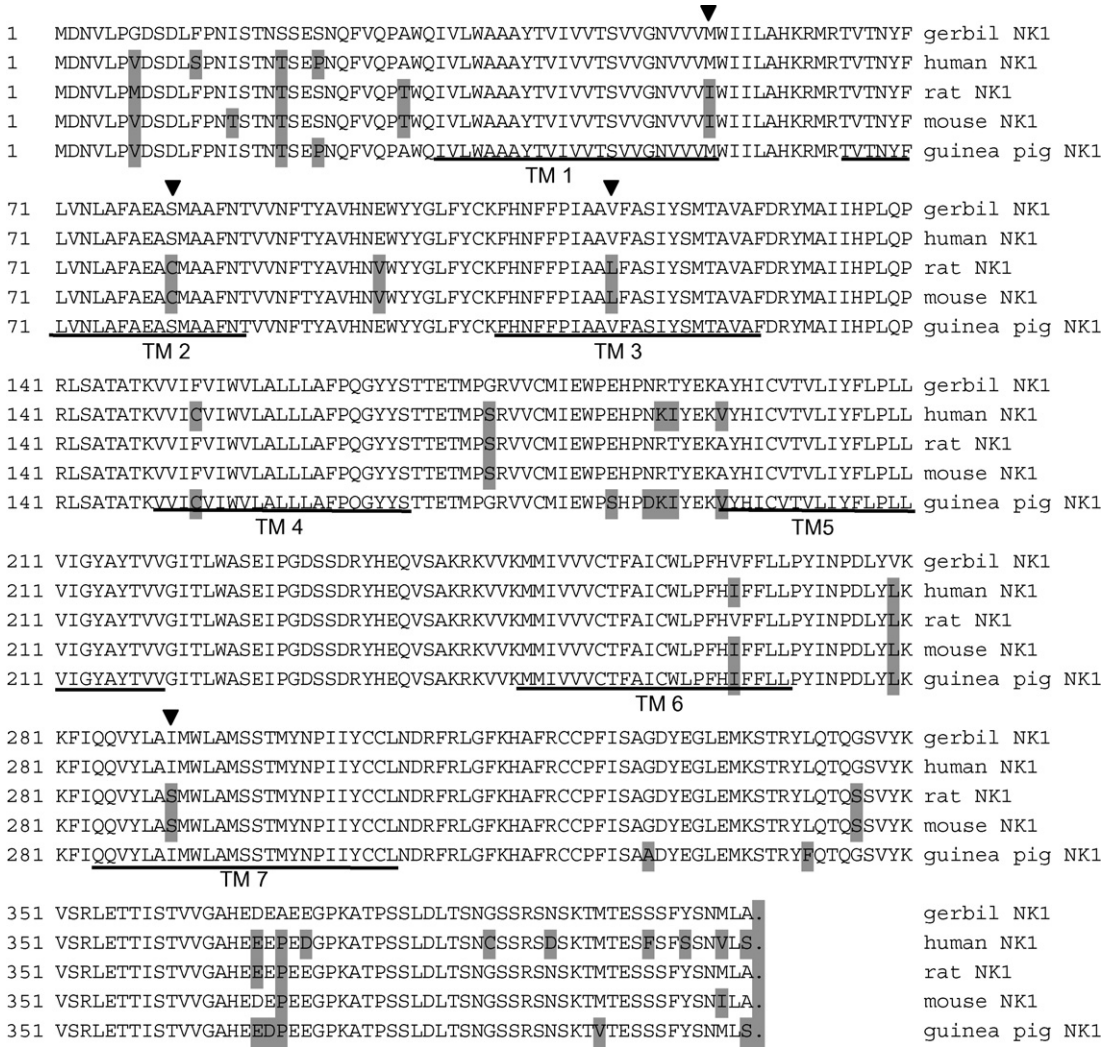

Fig. 2 – Amino acid sequence alignments of gerbil (cloned), human (P25103), mouse (P30548), rat (P14600) and guinea pig (P30547) NK_1R. Amino acids that differ from the gerbil NK_1R are shaded. Mutations performed in this study are marked with arrows (▼) and the transmembrane regions (TM1–TM7) are underlined.

3. Results

3.1. Primary structure of gerbil NK_1R

Cloned amino acid sequence of the gerbil NK_1R is shown, including comparisons with human, mouse (m), rat and guinea pig (gp) NK_1R sequences (Fig. 2). The gNK_1R has a slightly higher degree of overall homology towards rNK_1R and mNK_1R (~97%) than towards its more putative pharmacologically related species hNK_1R and $gpNK_1R$ (~95%) (Table 2). However, in the Tm regions, only three amino acid differed between gerbil and human NK_1R (one each in Tm 4–6, Table 3). Residues 116 and 290, previously reported to be important for evaluation of species-selective antagonist binding, were identical in the gerbil and human sequence. Four amino acid differed between gerbil and rat (one each in Tm 1, 2, 3 and 7), including residues 116 and 290 (Table 3). Since the 4 amino acid that differed between gerbil and rat NK_1R were identical between gerbil and human (Table 3), we chose to investigate the importance of these amino acid for potency of small molecular antagonists using site-directed mutagenesis (see also Table 1).

3.2. Agonist affinity and potency

Saturation binding experiments were performed in cell lines transfected with hNK_1R, rNK_1R and gNK_1R, respectively. The K_d-values for ^{3}H-SarMet SP were 2.1 ± 0.6, $n = 3$ and 3.1 ± 0.7 nM, $n = 4$ at human and gNK_1R while the affinity for rNK_1R was 12.4 ± 3.3 nM, $n = 3$. The maximal number of receptors (B_{max}) expressed in human-, gerbil- and rat CHO-NK_1R were in the range 4200–9700 fmol/mg protein, $n = 3$–4. The functional potencies of SP, ASMSP, NKA and pro7NKB at hNK_1R, rNK_1R and gNK_1R are shown in Table 4 and the concentration–response curves are shown in Fig. 3. The rank order was SP $\geq$ ASMSP $\geq$ NKA $\ggg$ pro7NKB for NK_1R of rat and human. All four agonists had comparable potency for hNK1 and rNK1 receptor. Surprisingly, all agonists (NKA in particular) were less potent at gNK_1R (by 7–85 times) compared to hNK_1R and rNK_1R (Table 4).

Fig. 4 shows saturation binding of ^{3}H-SarMetSP to the wild type gNK_1R and to the different mutated gNK_1R. B_{max}-values differed markedly probably reflecting the variation in protein properties caused by the introduced mutations which may result in different NK_1R expression levels. However, the affinity of ^{3}H-SarMetSP was not affected by the different mutations (Fig. 4). Also, SP had similar potency (EC_{50}-values) at the wt gNK_1R (0.18 ± 0.13 nM) as compared to the mutated gNK_1Rs (0.17 ± 0.10 nM, mut 3; 0.36 ± 0.22 nM, mut 4 and 0.28 ± 0.16 nM, mut 5, $n \geq 4$).

Table 3 – Positions in transmembrane regions 1–7 of NK_1R where amino acids differ between human, gerbil and rat

TM region	AA pos	Gerbil/human	Gerbil/rat	Human/rat
TM1	54		**Met/Ile**	Met/Ile
TM2	80		**Ser/Cys**	Ser/Cys
TM3	116		**Val/Leu**	Val/Leu
TM4	152	Phe/Cys		Cys/Phe
TM5	195	Ala/Val		Val/Ala
TM6	266	Val/Ile		Ile/Val
TM7	290		**Ile/Ser**	Ile/Ser

The performed mutations in the gerbil NK_1R and the localization of the exchanged amino acid are shown in bold. The position of the performed gerbil to rat mutations are pos 54 (mut 1), pos 80 (mut 2), pos 116 (mut 3), pos 290 (mut 4) and the combined mutation (mut 5 = mut 1 + 2 + 3 + 4).

3.3. Antagonist affinity and potency

CP99994 and ZD6021 had similar affinities for gNK_1R and hNK_1R (pK_i: 9.4–9.6) while having >500-fold lower affinity for rNK_1R (pK_i: 6.4–6.8) (Table 5). The potency of the antagonists (pK_B-values) corresponded with their respective affinities but the pK_i-values were in all cases higher (Table 5). In addition, the putative rat NK_1R-preferring antagonist RP67580 had comparable affinity and potency at hNK_1R and rNK_1R while being slightly less potent at gNK_1R (Table 5).

CP99994 and ZD6021 had similar potency at human, wt gerbil NK_1R (Table 6) and mutants 1 and 2 (data not shown). Their potency decreased 10–20-fold in mutants 3 (Val116-Leu) and 4 (Ile290Ser) and decreased further (60-fold) when combined mutations were introduced (Table 6). In contrast, RP67580 had the opposite profile, manifested as low potency for wt gNK_1R followed by an increased potency (10-fold) for mutation 3 (Val116Leu). Mutation 4 did not seem to affect the potency of RP67580. In the combined mutation (mutation 5), the potency of RP67580 ($pK_B = 7.7$) was similar to wt rat NK_1R ($pK_B = 7.3$) (compare Tables 5 and 6).

Table 2 – Sequence homology of NK_1R orthologues

	Human (%)	Mouse (%)	Rat (%)	Guinea pig (%)
Gerbil	95	96	97	95
Human		94	94	96
Mouse			98	94
Rat				94
Guinea pig				

The overall receptor homology is quite consistent among the various species with the rat and mouse NK_1R having the highest homology.

Table 4 – Potency of SP, NKA, Pro7NKB and ASMSP at stimulating NK_1R-mediated increases in intracellular Ca^{2+} (fluorescence units) in CHO cells transfected with human, gerbil or rat NK_1R

Agonist	Human NK_1R	Gerbil NK_1R	Rat NK_1R
Substance P	0.03 ± 0.01	0.22 ± 0.14	0.03 ± 0.02
NKA	0.06 ± 0.02	3.41 ± 1.9	0.04 ± 0.03
Pro7NKB	371 ± 200	3587 ± 2496	226 ± 108
ASMSP	0.03 ± 0.02	0.87 ± 0.60	0.06 ± 0.06

Results are mean EC_{50} (nM) $\pm$ S.D., $n \geq 3$.

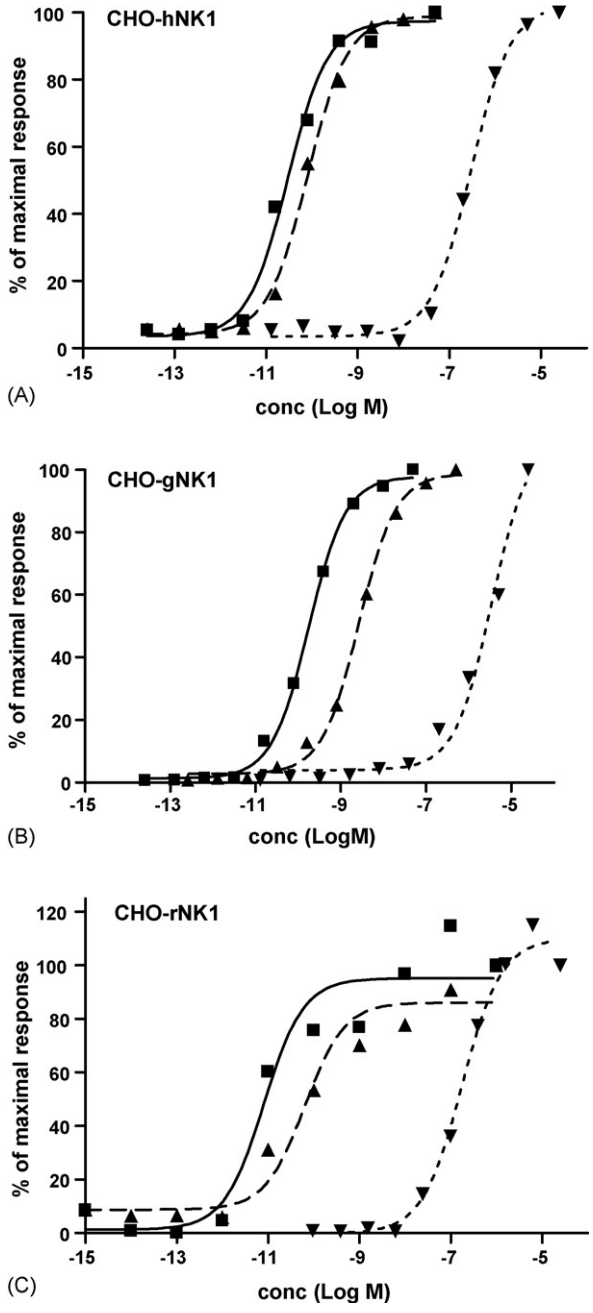

Fig. 3 – Concentration response curves for SP (■), NKA (▲) and Pro7NKB (▼) on NK_1R-CHO evoked increases in intracellular Ca^{2+}. Human NK_1R (A), gerbil NK_1R (B) and rat NK_1R (C).

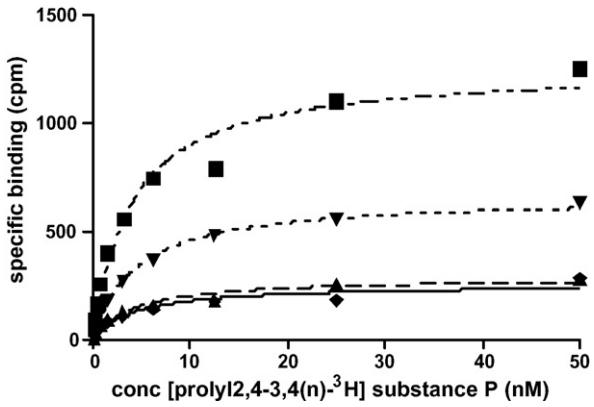

Fig. 4 – Saturation binding curves showing specific binding of ^{3}H-SarMetSP to wild type gerbil NK_1R (■), mutation 3 (Val116Leu) (▲), mutation 4 (Ile290Ser) (▼) and the combined mutation 5 (Met54Ile, Ser80Cys, Val116Leu and Ile290Ser) (◆).

3.4. *Inhibitory effect of NKR antagonists in vivo*

The ASMSP, 10 pmol (ED_{90} dose) induced behaviour effect in GFT was inhibited 60–70% by pre-treatment with 1 μmol/kg CP99994 (s.c.) or by 10 μmol/kg ZD6021 (i.p.) (Table 7). In contrast, RP67580 at 10 μmol/kg (i.p.) did not significantly affect the GFT response, despite reaching higher brain concentrations than ZD6021 (Table 7).

4. Discussion

Gerbils are often used when evaluating the effects of NK_1R antagonists *in vivo* since they are claimed to have similar antagonist pharmacology as the human NK_1R. The current study reveals the primary structure of the gerbil NK_1R and confirms that three NK_1R antagonists bind the gNK_1R and the hNK_1R with comparable affinity and also have similar degrees of functional potency. Finally, we demonstrate that the gNK_1R shares key amino acid with the hNK_1R that are crucial for antagonist function and play an important in role in explaining differences in NK_1R species selectivity.

The gNK_1R has high homology with the human NK_1R (95%). However, the overall homology is of the same degree between rNK_1R and hNK_1R (94%). Thus, merely comparing the degrees of overall homology does not predict potential species

Table 5 – Comparison between binding affinity (pK_i) and functional potency (pK_B) of NK_1R antagonists

Compound	Human NK_1R		Gerbil NK_1R		Rat NK_1R	
	pK_i	pK_B	pK_i	pK_B	pK_i	pK_B
ZD6021	9.6 ± 0.2	8.6 ± 0.4	9.6 ± 0.2	9.0 ± 0.2	6.8 ± 0.1	<6
CP99994	9.4 ± 0.1	8.7 ± 0.2	9.2 ± 0.2	8.9 ± 0.3	6.4 ± 0.1	5.9 ± 0.2
RP67580	8.0 ± 0.1	7.1 ± 0.4	6.6 ± 0.3	6.5 ± 0.2	7.4 ± 0.1	7.3 ± 0.4

For determination of antagonist binding affinity to NK_1R ^{3}H-SarMet SP was used as radioligand and for determination of antagonist potency, SP-evoked increases in intracellular Ca^{2+} were monitored. Binding experiments were performed in membranes and *in vitro* function was performed in CHO cells transfected with NK_1R of different species. Results are mean pK_B and $pK_i \pm$ S.D., $n \geq 3$.

Table 6 – Potency values (pK_B) of NK_1R antagonists at inhibiting SP-evoked increases in intracellular Ca^{2+} in cells transfected with wild type or mutated gerbil NK_1R

Compound	Gerbil NK_1R wt	Mutation 3 (Val116Leu)	Mutation 4 (Ile290Ser)	Mutation 5 (1 + 2 + 3 + 4)
ZD6021	8.9 ± 0.2	7.6 ± 0.2	7.6 ± 0.1	7.2 ± 0.2 (n = 2)
CP99994	9.0 ± 0.1	8.0 ± 0.3	7.7 ± 0.2	7.2 ± 0.1
RP67580	6.3 ± 0.6	7.4 ± 0.7	6.5 ± 0.7	7.7 ± 0.4

Results are mean pK_B ± S.D., $n \geq 3$ unless indicated otherwise.

Table 7 – Inhibitory effect of CP99994, ZD6021 and RP67580 on ASMSP-evoked GFT response

Compound	Dose (μmol/kg)	Inhibition (%)	Brain levels (nmol/kg w.w.)
ZD6021	10 (i.p.)	69 ± 11	85 ± 8
CP99994	1 (s.c.)	62 ± 5	508 ± 40
RP67580	10 (i.p.)	15 ± 19	148 ± 4

Results are mean ± S.E.M., n = 3–6.

differences in pharmacology. Tm regions are often targets for small molecule antagonists [34]. Three amino acid in the Tm regions (residues 152, 195 and 266) differed between gNK_1R and hNK_1R. These residues are not likely to play a major role in antagonist function since the potency and affinity of the antagonists evaluated at hNK_1R and gNK_1R were the same between species. Discrepancies in affinity and potency values may relate to the different methods used, the Ca^{2+} assay includes a short incubation of SP in order to capture the intra cellular mobilization of Ca^{2+} while the binding assay relates to an equilibrium situation.

Four amino acids in the Tm regions differed between gNK_1R and rNK_1R. The fact that two of these residues were 116 and 290 (identical between gNK_1R and hNK_1R) is of interest since it has previously been elegantly shown that these NK_1R residues play a key role in regard to species selectivity of antagonist binding [15,17,18,19,35]. The present study demonstrates that these residues not only play a key role for antagonist binding, but also for antagonist function at the gNK_1R since the antagonists CP99994 and ZD6021 had similar affinity and potency for the wild-type receptor while the potency of the antagonists decreased markedly when mutations were introduced at positions 116 and 290. Mutations at positions 54 and 80, residues identical between human and gerbil but differ in rat, had no effect on antagonist potency, suggesting that these residues play a minimal role for antagonist function and binding. None of the mutations introduced in gNK_1R affected the affinity or potency of substance P indicating that these substitutions do not cause large-scale distortion of the receptor conformation. Other residues have been implicated in the binding of small molecule antagonists to NK1 receptors such as His-165, His-197, His-265, Phe-268 and Tyr-287 [35–37]. These residues appear to be highly conserved among species, including gerbils, and hence do not explain species-related differences in antagonist pharmacology.

The suggested binding site in the NK_1R used by the compounds is illustrated in the rhodopsin homology model (Figs. 5 and 6) [32]. It is noteworthy that residues 54 and 80 are distant from the center of the antagonist binding pocket, while positions 116 and 290 are much closer, making interactions between receptor and antagonist more likely.

Residue 116 consists of the hydrophobic amino acid valine in the human/gerbil NK_1R sequence. Replacing valine in the gNK_1R with the rat homolog leucine, also a hydrophobic amino acid, markedly decreased the potency of CP99994 and ZD6021 (10- and 20-fold, respectively). This conservative substitution in the hNK_1R has been shown to cause decreased antagonist affinity depending on the compound examined [15,18,19]. The

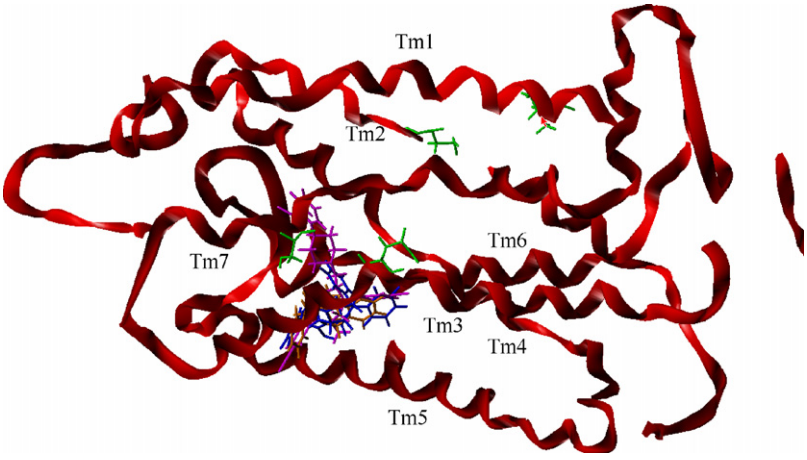

Fig. 5 – Chemical structures docked into the ligand-supported rhodopsin NK_1R homology model. The site specific mutation sites (Met54Ile, Ser80Cys, Val116Leu and Ile290Ser) are shown in green. Position 116 and 290 cover the site where the antagonists bind. Position 54 and 80 are by far more distant from the binding site. The three NK_1R antagonists ZD6021, RP67580 and CP99994 are shown in the active binding site. Tm region are indicated. (For interpretation of the references to colour in this figure legend, the reader is referred to the web version of the article.)

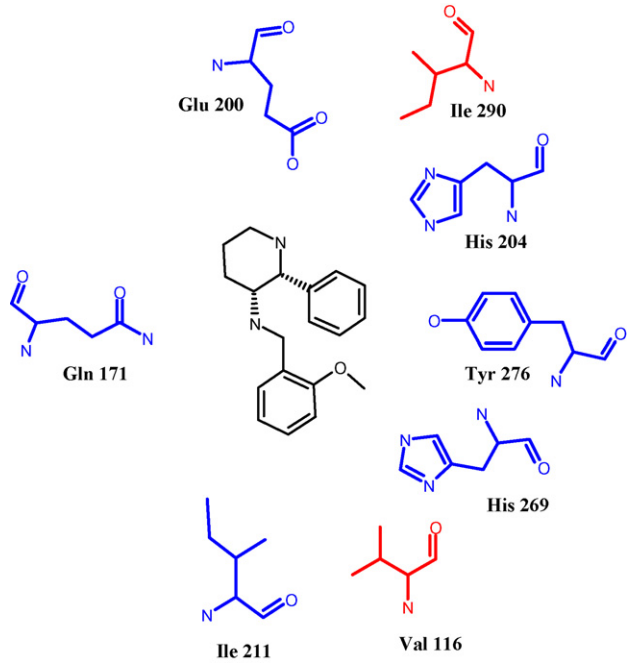

Fig. 6 – Interactions of CP99994 in the ligand supported postulated NK_1R ligand interaction model. CP99994 is shown together with the putative binding sites recognized in the homology model (Fig. 5, see also [34]). In mutation 3, Val116 was mutated to Leu116. In mutation 4 Ile290 was exchanged with Ser290. The mutated amino acids are indicated in red and connecting amino acid are in blue. (For interpretation of the references to colour in this figure legend, the reader is referred to the web version of the article.)

affinity of CP99994 appears to be affected by this mutation at site 116 in the hNK_1R [19], which is in line with our data when introducing the same mutation in the gNK_1R. This conservative mutation results in small changes in the physicochemical properties of the side chain and might induce a slight modification in receptor conformation of the binding site, also discussed by [19]. Multiple mutational data have been used to characterize the amino acid residues essential for binding of CP99994, which are high lighted in Fig. 6 [35,38–45].

Mutating Val-116 to Leu-116 does not alter the hydrophobicity between Ile-211 and His-269. However, sterical hindrance may occur with the larger amino acid Leu-116 is present, and thereby affect binding and potency of NK_1R antagonists. The present study also demonstrates that the importance of residue 116 is extended to the structurally different NK_1R antagonist ZD6021.

Residue 290 consists of the hydrophobic amino acid Ile in the gerbil/human NK_1R sequences, while rat residue 290 contains the smaller hydrophilic amino acid serine. Thus the mutation Ile290Ser produces more drastic changes in the physicochemical nature of this residue. Indeed, this mutation in the hNK_1R causes large decreases in affinity for human-preferring NK_1R antagonists [15,16,18,19]. In the current study, this mutation in the gNK_1R reduced the potency of CP99994 and ZD6021 by 20-fold. The results with CP99994 are in agreement with a previous report which introduced the same mutation in the hNK_1R [19]. Residue 290 is close to Glu-200 and His-204, both being hydrophilic charged amino acids (Fig. 6). The Ile290Ser mutation may induce tilting of the TM7 helix and thereby create new hydrogen bonding which most certainly affects binding and potency of NK_1R antagonists.

When mutations were introduced in all Tm residues differing between rat and gerbil (positions 54, 80, 116 and 290) the potency of CP99994 and ZD6021 was lower (60-fold) than when single mutations were introduced in positions 116 or 290 (10–20-fold). Despite replacing the four residues with rat homologs, the potency was still higher than at wild-type rNK_1R. Thus, it cannot be excluded that additional residues may contribute in determining the species difference between rat and gerbil.

The current study also shows that RP67580 binds human and rat NK_1R to a similar degree, while having a slightly lower affinity for gNK_1R. Previous reports show that RP67580 does not fully stretch into the gerbil/human NK_1R binding pocket and therefore species differences are not as prominent [35,46,47]. These results are contradictory to others who have reported that RP67580 has a 5-fold [15,19] higher affinity for the rNK_1R than for the hNK_1R. Our data suggest that RP67580 has approximately equal affinity and functional potency at human and rat NK_1R and should therefore not be regarded as a rat-preferring or rat-selective NK_1R antagonist.

The *in vitro* pharmacology of the gNK_1R was also confirmed *in vivo* by monitoring gerbil foot tap (GFT) responses. CP99994 and ZD6021 inhibited ASMSP-evoked GFT to a similar degree at the doses indicated. RP67580 had no significant inhibitory effect despite being present in the brain at similar levels as ZD6021. This is most likely explained by the weak potency at gNK_1R described in the *in vitro* studies. Our results with RP67580 are in agreement with [24].

The current study mainly addresses sequence differences in the Tm regions, although differences between gNK_1R and rNK_1R, as well as hNK_1R, were found in other regions of the NK_1R. These regions are not generally considered to be important for NK_1R antagonist function. However, they may play an important role in agonist binding and G-protein coupling. Indeed, the agonists used in the current study had lower potency at gNK_1R which may be due to amino acid differences in these regions. Huang et al. [37] indicated that residues 85, 89, 96 and 287 are required for high affinity binding of tachykinins. These residues are conserved between human, rat and gerbil, thus not explaining the discrepancy in agonist potency demonstrated in the present study. The lower potency at the gNK_1R may reflect a less efficient coupling to G-proteins since affinity values for SarMet SP were similar between gNK_1R and hNK_1R. Huang et al. [37] also identified residues 78 and 205 as important for the receptor activation process. These residues were also found to be conserved between species.

In conclusion, gNK_1R has high homology with hNK_1R and shares key residues (116 and 290) important not only for binding but also for functional activity of the potent human/gerbil-preferring NK_1R antagonists ZD6021 and CP99994. By contrast, the less-active antagonist RP67580 does not discriminate between NK_1R of the different species. Thus, the results from the current study lend further support to the use

of gerbils as an animal species to characterize the pharmacology of NK_1R antagonists.

Moreover, the present findings reveal that the classification of NK_1R into the two sub-families, human/gerbil and rat is related to rather subtle differences in amino acid residues in the binding site. Hence, species differences are to a great extent dictated by antagonist binding regions and structure and to a lesser extent by the sequence difference in the receptor itself.

REFERENCES

[1] Severini C, Improta G, Falconieri-Erspamer G, Salvadori S, Erspamer V. The tachykinin peptide family. Pharm Rev 2002;54:285–322.

[2] Patacchini R, Lecci A, Holzer P, Maggi CA. Newly discovered tachykinins raise new questions about their peripheral roles and the tachykinin nomenclature. Trends Pharmacol Sci 2004;25:1–3.

[3] Maggi CA, Petacchini R, Rovero P, Giachetti A. Tachykinin receptors and tachykinin receptor antagonists. J Autonom Pharmacol 1993;13:23–93.

[4] Maggi CA. Tachykinins in the autonomic nervous system. Pharm Res 1996;33:161–70.

[5] Pennefather JN, Alessandro L, Candenas ML, Patak E, Pinto FM, Maggi CA. Tachykinins and tachykinin receptors: a growing family. Life Sci 2004;74:1445–63.

[6] Kramer MS, Cutler N, Feighner J, Shrivastava R, Carman J, Sramek JJ, et al. Distinct mechanism for anti-depressant activity by blockade of central substance P receptors. Science 1998;281:1640–5.

[7] Leroy V, Mauser P, Gao Z, Peet NP. Neurokinin receptor antagonists. Exp Opin Invest Drugs 2000;9:735–46.

[8] Holzer P, Holzer-Petsche U. Tachykinin receptors in the gut: physiological and pathological implications. Curr Opin Pharmacol 2001;1(6):583–90.

[9] Lecci A, Valenti C, Maggi CA. Tachykinin receptor antagonists in irritable bowel syndrome. Curr Opin Invest Drugs 2002;3:589–601.

[10] Duffy RA. Potential therapeutic targets for neurokinin-1 receptor antagonists. Exp Opin Emerg Drugs 2004;9:9–21.

[11] Humphrey JM. Medicinal chemistry of selective neurokinin antagonists. Curr Top Med Chem 2003;3:1423–35.

[12] Saria A. The tachykinin NK1 receptor in the brain: pharmacology and putative functions. Eur J Pharmacol 1999;375:51–60.

[13] Beresford IJM, Birch PJ, Hagan RM, Ireland SJ. Investigation into species variants in tachykinin NK1 receptors by use of the non-peptide antagonist, CP-96,345. Br J Pharmacol 1991;104:292–3.

[14] Appell KC, Fragale BJ, Loscig J, Singh S, Tomczuk BE. Antagonists that demonstrate species differences in neurokinin-1 receptors. Mol Pharmacol 1992;41(4):772–8.

[15] Fong TM, Yu H, Strader CD. Molecular basis for the species selectivity of the neurokinin-1 receptor antagonist CP-96,345. J Biol Chem 1992;267:25668–71.

[16] Sachais BS, Krause JE. Both extracellular and transmembrane residues contribute to the species selectivity of the neurokinin-1 receptor antagonist WIN 51708. J Pharmacol Exp Ther 1994;46:122–8.

[17] Sachais BS, Snider RM, Lowe JA, Krause JE. Molecular basis for the species selectivity of the substance P antagonist CP-96,345. J Biol Chem 1993;268:2319–23.

[18] Jensen CJ, Gerard NP, Schwartz TW, Gether U. The species selectivity of chemically distinct tachykinin nonpeptide antagonists is dependent on common divergent residues of the rat and human neurokinin-1 receptors. Mol Pharmacol 1994;45(2):294–9.

[19] Pradier L, Habert-Ortoli E, Emile L, Le Guern J, Loquet I, Bock M-D, et al. Molecular determinants of species selectivity of neurokinin type 1 receptor antagonists. Mol Pharmacol 1995;47:314–21.

[20] Bristow LJ, Young L. Chromodacryorrhea and repitive hind paw tapping: models of peripheral and central tachykinin NK1 receptor activation in gerbils. Eur J Pharmacol 1994;253:245–52.

[21] Rupniak NMJ, Tattersall FD, Williams AR, Rycroft W, Carlson EJ, Cascieri MA, et al. In vitro and in vivo predictors of the anti-emetic activity of tachylinin NK1 receptor antagonists. Eur J Pharmacol 1997;326:201–9.

[22] Rumsey WL, Aharony D, Bialecki RA, Abbott BM, Barthlow HG, Caccese R, et al. Pharmacological characterization of ZD6021: a novel, orally active antagonist of the tachykinin receptors. J Pharmacol Exp Ther 2001;298:307–15.

[23] Megens AAHP, Ashton D, Vermeire JCA, Vermonte PCM, Hens KA, Hillen LC, et al. Pharmacological profile of (2R-*trans*)-4-[1-[3,5-bis(trifluoromethyl)benzoyl]-2-(phenylmethyl)-4-piperidinyl]-*N*-(2,6-dimethylphenyl)-1-acetamide (*S*)-hydroxybutanedioate (R116301), an orally and centrally active neurokinin-1 receptor antagonist. J Pharmacol Exp Ther 2002;302:696–709.

[24] Rupinak N, Carlsson EJ, Shepard S, Bentley G, Williams AR, Hill A, et al. Comparison of the functional blockade of rat substance P (NK1) receptors by GR205171, RP67580, SR140333 and NKP-608. Neuropharmacology 2003;45:231–41.

[25] Duffy RA, Varty GB, Morgan CA, Lachowicz JE. Correlation of neurokinin (NK) 1 receptor occupancy in gerbil striatum with behavioural effects of NK1 antagonists. J Pharmacol Exp Ther 2002;301:536–42.

[26] Varty GB, Cohen-Williams ME, Morgan CA, Pylak U, Duffy RA, Lachowicz JE, et al. The gerbil elevated plus-maze II: anxiolytic-like effects of selective neurokinin NK1 receptor antagonists. Neuropsychopharmacology 2002;27:371–9.

[27] Varty GB, Cohen-Williams ME, Hunter JC. The antidepressant-like effects of neurokinin NK1 receptor antagonists in a gerbil tail suspension test. Behav Pharmacol 2003;14:87–95.

[28] Bernstein PR, Aharony D, Albert JS, Andisik D, Barthlow HG, Bialecki R, et al. Discovery of novel, orally active dual NK1/NK2 antagonist. Bioorg Med Chem Lett 2001;11:2769–73.

[29] Chandrasekhar S, Mohanty PK. Stereoselective synthesis of (+)-CP-99994: a substance P non-peptide antagonist. Tetrahedron Lett 1999;40:5071–2.

[30] Peyronel AT, Moutonnier C, Garret C. Synthesis of RP-67,580, a new potent non-peptide substance P antagonist. Bioorg Med Chem Lett 1992;2:37–40.

[31] Bradford M. A rapid and sensitive method for the quantitation of microgram quantities of protein utilizing the principle of protein–dye binding. Anal Biochem 1976;72:248.

[32] Teller DC, Okada T, Behnke CA, Palczewski K, Stenkamp RE. Advances in determination of a high-resolution three-dimensional structure of rhodopsin, a model of G-protein-coupled receptors (GPCRs). Biochemistry 2001;40:7761–72.

[33] Cheng Y, Prsoff WH. Relationship between the inhibition constant (K_i) and the concentration of inhibitor, which cause 50 percent inhibition (IC50) of an enzymatic reaction. Biochem Pharmacol 1973;22:3099–108.

[34] Schwartz TW. Locating ligand-binding sites in 7TM receptors by protein engineering. Curr Opin Biotechnol 1994;5:434–44.

[35] Evers A, Klebe G. Successful virtual screening for a submicromolar antagonist of the neurokinin-1 receptor.

Based on a ligand-supported homology model. J Med Chem 2004;47:5381–92.
[36] Fong TM, Yu H, Cascieri MA, Underwood D, Swain CJ, Strader CD. The role of histidine 265 in antagonist binding to the neurokinin-1 receptor. J Biol Chem 1994;269:2728–32.
[37] Huang RRC, Yu H, Stocker CD, Fong TM. Interaction of substance P with the second and seventh transmembrane domains of the neurokinin-1 receptor. Biochemistry 1994;33:3007–13.
[38] Lundström K, Hawcock AB, Vargas A, Ward P, Thomas P, Naylor A. Effect of single point mutations of the human tachykinin NK1 receptor on antagonist affinity. Eur J Pharmacol 1997;337:73–81.
[39] Boks GJ, Tollenaere JP, Kroon J. Possible ligand-receptor interactions for NK1 antagonists as observed in their crystal structures. Bioorg Med Chem 1997;5:535–47.
[40] Swain CJ, Seward EM, Cascieri MA, Fong TM, Herbert R, MacIntyre DE, et al. Identification of a series of 3-(benzyloxy)-1-azabicyclo[2.2.2]octane human NK1 antagonists. J Med Chem 1995;38:4793–805.
[41] Elliott JM, Cascieri MA, Chicchi G, Davies S, Kelleher FJ, Kurtz M, et al. Serine derived NK1 antagonists. 1. The effect of modifications to the serine substituents. Bioorg Med Chem Lett 1998;8:1845–50.
[42] Elliott JM, Broughton H, Cascieri MA, Chicchi G, Huscroft IT, Kurtz M, et al. Serine derived NK1 antagonists. 2. A pharmacophore model for arylsulfonamide binding. Bioorg Med Chem Lett 1998;8:1851–6.
[43] Takeuchi Y, Shands EFB, Beusen DD, Marshall GR. Derivation of a three-dimensional pharmacophore model of substance P antagonists bound to the neurokinin-1 receptor. J Med Chem 1998;41:3609–23.
[44] Jacoby E, Boudon A, Kucharczyk N, Michel A, Fauchere JL. A structural rationale for the design of water soluble peptide-derived neurokinin-1 antagonists. J Recep Signal Transduction Res 1997;17:855–73.
[45] Vedani A, Briem H, Dobler M, Dollinger H, McMasters DR. Multiple-conformation and protonation-state representation in 4D-QSAR: the neurokinin-1 receptor system. J Med Chem 2000;43:4416–27.
[46] Poulsen A, Björholm B, Gundetofte K, Pogozheva ID, Liljefors T. Pharmacophore and receptor models for neurokinin receptors. J Comput-Aided Mol Design 2003;17:765–83.
[47] Poulsen, Bjornholm B, Gundertofte K, Pogozheva ID, Liljefors T. Pharmacophore and receptor models for neurokinin receptors. J Computer-Aided Mol Design 2004;17(11):765–83.